International Journal of Automotive Technology, Vol. 19, No. 2, pp. 359–367 (2018)
DOI 10.1007/s12239–018–0034–z

pISSN 1229–9138/ eISSN 1976–3832

DESIGN AND EVALUATION OF ROBUST COOPERATIVE ADAPTIVE CRUISE CONTROL SYSTEMS IN PARAMETER SPACE

Mümin Tolga Emirler[1)*], Levent Güvenç[2, 3, 4)] and Bilin Aksun Güvenç[2, 3)]

[1)]Department of Mechanical Engineering, Istanbul Okan University, Istanbul 34959, Turkey
[2)]Automated Driving Lab in the Center for Automotive Research, The Ohio State University, Columbus, OH 43210, USA
[3)]Department of Mechanical and Aerospace Engineering, The Ohio State University, Columbus, OH 43210, USA
[4)]Department of Electrical and Computer Engineering, The Ohio State University, Columbus, OH 43210, USA

(Received 13 February 2017; Revised 20 June 2017; Accepted 20 July 2017)

ABSTRACT–This paper is on the design of cooperative adaptive cruise control systems for automated driving of platoons of vehicles in the longitudinal direction. Longitudinal models of vehicles with simple dynamics, an uncertain first order time constant and vehicle to vehicle communication with a communication delay are used in the vehicle modeling. A robust parameter space approach is developed and applied to the design of the cooperative adaptive cruise control system. D-stability is chosen as the robust performance goal and the feedback PD controller is designed in controller parameter space to achieve this D-stability goal for a range of possible longitudinal dynamics time constants and different values of time gap. Preceding vehicle acceleration is sent to the ego vehicle using vehicle to vehicle communication and a feedforward controller is used in this inter-vehicle loop to improve performance. Simulation results of an eight vehicle platoon of heterogeneous vehicles are presented and evaluated to demonstrate the efficiency of the proposed design method. Also, the proposed method is compared with a benchmark controller and the feedback only controller. Time gap regulation and string stability are used to assess performance and the effect of the vehicle to vehicle communication frequency on control system performance is also investigated.

KEY WORDS : Cooperative adaptive cruise control, Parameter space control system design, D-stability

1. INTRODUCTION

Connected vehicle technologies based on vehicle-to-vehicle (V2V) communication are expected to be present in series production vehicles as early as 2017. Similarly, automated driving vehicles are expected to be series produced after the year 2020 according to recent reports. Cooperative Adaptive Cruise Control (CACC) is the simplest automated driving technology that uses V2V communication. It is expected to be in series production vehicles within the 2017 ~ 2020 period. CACC uses V2V communication of preceding vehicle acceleration in order to improve the spacing of vehicles in convoy driving (Güvenç *et al*., 2012). CACC can also be viewed as an improved version of adaptive cruise control (ACC) that will be easily implementable after series production of cars with V2V communication. Dedicated Short Range Communication (DSRC) based on the IEEE 802.11p standard is used in the V2V modem in CACC as it is a safety critical system.

Vehicles in which CACC will be applied will have different longitudinal vehicle dynamics model parameters. Even the same type of vehicle may have different parameters due to differences in loading including passengers, the variable velocity of operation and differences in road surface adhesion characteristics. Accordingly, a robust control design approach has to be used in CACC design.

There have been a few attempts in the literature on robust design of CACC systems. In Trudgen and Mohammadpour (2015), a robust H_∞ controller for CACC was designed using loop shaping design methodology. Then, model reduction techniques were employed to reduce the order of the designed controller. In Maschuw *et al*. (2008), the design requirements of a longitudinal control of vehicle platoon were expressed as a mixed H_2/H_∞ problem as one set of linear matrix inequalities that are solved for the controller. In Gao *et al*. (2017), a decoupled robust control strategy was proposed and the performance of the proposed control system was compared with a non-robust controller by the help of simulations. The necessity of the robust stability of vehicular platoon when designing control system was shown as a result of this study.

Robust control systems should be designed to handle model uncertainties and external disturbances and to provide control performance requirements. There are several

**Corresponding author.* e-mail: tolga.emirler@okan.edu.tr

methods for robustness analysis and robust control design in the literature. Two major approaches are the parameter space method and frequency domain approaches like H_∞ robust control. Frequency domain approaches treat unstructured uncertainty and they are developed generally for multi input multi output systems. On the other hand, parameter space method mainly used for structured uncertainties. The parameter space approach can be used to determine a set of coefficients for a given controller structure which simultaneously stabilize a finite number of plants. The set of parameters for which the characteristic polynomial is Hurwitz-stable can be mapped into controller parameter space by solving the polynomial parameterized by the frequency. Along with Hurwitz stability, the method has been extended to D-regions for treating relative stability and bandwidth constraints. In practice, the controller pairs can be selected by using 2D plots which shows the (Hurwitz or D-) stable and unstable regions. The other details of the parameter space approach can be found in Ackermann *et al*. (2002) and Güvenç *et al*. (2017).

A comparison of the parameter space approach and frequency domain approaches like H_∞ can be found in Güvenç and Ackermann (2001), Demirel and Güvenç (2010). Some of the results can be summarized as follows. The advantages of the parameter space approach in comparison with H_∞ methods are: (i) The ease of visualization due to the graphical representation of the solution in the parameter space approach, (ii) The determination of a solution region rather than one specific solution, (iii) The determination of controller parameters that guarantee robust performance, (iv) Obtaining fixed structure low order controller filters that are easily implementable. There are also some shortcomings of the parameter space approach in comparison to H_∞ methods such as: (i) The method can simultaneously accommodate the design of only two to three controller parameters due to its graphical display of the solution region, (ii) The method does not result in a single analytical solution. The main contribution and novelty of this paper is the presentation and evaluation of a robust controller for CACC design based on the parameter space approach combined with a feedforward controller and the evaluation of this controller using V2V communication frequency along with the more standard time gap regulation and string stability methods. The parameter space design was chosen based on the above comparison of robust control methods and due to the fact that they have not been used before for CACC controller design. The parameter space based CACC design approach presented here is easy to implement and design as it uses low order fixed structure controllers. Simple longitudinal dynamics models with uncertain first order dynamics are used.

The outline of the rest of the paper is as follows. The vehicle modeling used is presented in Section 2. The parameter space based robust CACC controller design procedure is given and the benchmark controller is introduced in Section 3. Simulation results from an eight vehicle convoy are presented in Section 4. In Section 5, CACC control system design is evaluated by means of time gap regulation, string stability and the effect of V2V communication frequency on system performance is investigated. The paper ends with conclusions and directions for future work in the last section.

2. VEHICLE MODELLING FOR CONTROLLER DESIGN AND TESTING

Cooperative adaptive cruise control (CACC) systems extend the capability of adaptive cruise control (ACC) systems by feeding the acceleration information of the preceding vehicle obtained via wireless communication. Using this extra information, the time gap in standard ACC systems can be reduced. ACC/CACC systems have upper and lower control levels. The upper level control is used for calculating the desired acceleration of the vehicle in the string. The lower level control contains throttle and brake sub-controllers which are employed to obtain the desired acceleration.

For the upper level controller design, a basic vehicle model can be considered as follows:

$$\ddot{x}_i = u \tag{1}$$

where $\ddot{x}_i$ shows the acceleration of the i^{th} vehicle in the convoy and u is the control input which is either throttle or brake command based on whether the control signal is positive or negative, respectively. Each vehicle is actually expected to follow the desired acceleration imperfectly due to the finite bandwidth of the lower level controller (Rajamani, 2011). This is represented by a first order lag in this paper as follows:

$$\ddot{x}_i = \frac{1}{\tau_i s + 1} u \tag{2}$$

where τ_i denotes the uncertain time constant of the longitudinal vehicle dynamics. As a result, the longitudinal dynamics of the vehicle i in the convoy can be represented by

$$G_i(s) = \frac{X_i(s)}{U(s)} = \frac{1}{s^2(\tau_i s + 1)} . \tag{3}$$

3. COOPERATIVE ADAPTIVE CRUISE CONTROL SYSTEM DESIGN

In general, CACC systems use a radar sensor and vehicle-to-vehicle (V2V) wireless communication using modems to maintain the desired headway gap. The radar provides relative distance and relative velocity difference between the preceding and ego vehicles which are used in the feedback ACC control part of the CACC. These systems use a radar sensor with a range of up to 200 m to detect preceding vehicles. The controller used can command

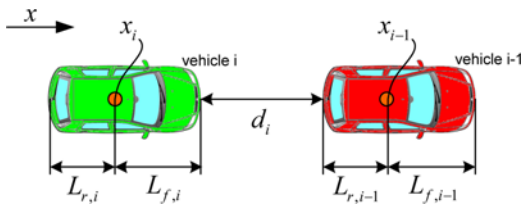

Figure 1. CACC equipped consecutive vehicles in the convoy.

throttle and brake (if needed) to adjust the desired time gap. On the other hand, the acceleration of the preceding vehicle is transmitted to the ego vehicle using V2V communication in the form of an IEEE 802.11p DSRC modem, which is employed for the feedforward part of the CACC system. Figure 1 shows two CACC equipped vehicles in a convoy. Different types of CACC sensor and communication structures can be employed. For example, all the required information for CACC (such the preceding vehicle's global position, velocity and acceleration) can be transmitted to the ego vehicle via V2V communication as was successfully done in Güvenç *et al*. (2012). In this structure, the ego vehicle's modem can obtain all the required information and the ego vehicle's computer compares the global position and velocity of the preceding vehicle with its global position and velocity to calculate the relative distance and velocity between two consecutive vehicles.

In the literature, the three different spacing policies of constant spacing, constant time gap and variable time gap can be found (Aksun Güvenç and Kural, 2006; Choi and Hedrick, 1995; Ioannou *et al*., 1993; Kural, 2006; Yanakiev *et al*., 1998). Constant spacing policy is not used in practice as the spacing needs to be changed based on vehicle speed. Constant spacing policy leads to string stability problems. Variable time gap is sometimes used for improving fuel efficiency by being less aggressive in accelerating the ego vehicle. Constant time gap is the preferred approach as it has better string stability and performance than a constant spacing policy. The constant time gap policy also results in the best performance and makes it easier to evaluate the performance of control as compared to a variable time gap. ACC systems implemented in series production vehicles use the constant time gap.

In this paper, we consider a constant time gap spacing policy for CACC where the desired relative distance between the front bumper of the *i*th vehicle and the preceding vehicle's rear bumper is defined as

$$d_{\mathrm{r,i}} = s_{\mathrm{i}} + \dot{x}_{\mathrm{i}} t_{\mathrm{hd,i}} \tag{4}$$

where $d_{\mathrm{r,i}}$ is the desired relative distance for the i^{th} vehicle, s_{i} is the standstill distance (at zero speed), $\dot{x}_{\mathrm{i}}$ is the speed of the i^{th} vehicle and $t_{\mathrm{hd,i}}$ is the time gap for the i^{th} vehicle.

For the sake of simplicity, the standstill distance s_{i} is taken as zero (s_{i} = 0) because it does not affect the dynamics of the vehicle and the analysis and design results presented in the rest of this paper. The actual relative distance between two consecutive vehicles can be written as follows according to Figure 1.

$$d_{\mathrm{i}} = x_{\mathrm{i-1}} - L_{\mathrm{r,i-1}} - (x_{\mathrm{i}} + L_{\mathrm{f,i}}) = x_{\mathrm{i-1}} - x_{\mathrm{i}} - L_{\mathrm{r,i-1}} - L_{\mathrm{f,i}} \tag{5}$$

where d_{i} is the actual relative distance between the two vehicles, $x_{\mathrm{i-1}}$ and x_{i} are the positions of the i-1^{th} and i^{th} vehicles, respectively. $L_{\mathrm{r,i-1}}$ is the distance between the rear bumper and the vehicle center of gravity for the i-1^{th} vehicle. $L_{\mathrm{f,i}}$ is the distance between the vehicle center of gravity and the front bumper for the i^{th} vehicle. In order to simplify the analysis, the vehicle lengths will be taken as zero in the rest of this paper for control system design, analysis and simulations resulting in

$$d_{\mathrm{i}} = x_{\mathrm{i-1}} - x_{\mathrm{i}}\,. \tag{6}$$

The general block diagram of the CACC system structure for a single vehicle is shown in Figure 2. CACC system can be considered as feedback-feedforward control system. ACC systems use feedback control alone to achieve the desired constant time gap. The feedforward controller is used when V2V communication is available to obtain the acceleration/deceleration signal of the preceding vehicle which improves performance by allowing smaller time gaps to be achieved. When the feedforward controller is used in this manner, the ACC system becomes a CACC system. In other words, the feedback and feedforward control parts ($C_{\mathrm{fb,i}}(s)$ and $C_{\mathrm{ff,i}}(s)$) constitute the overall CACC system. There have been some studies in the literature using this approach (Dey *et al*., 2016; Güvenç *et al*., 2012; Lidström *et al*., 2012; Naus *et al*., 2010; Ploeg *et al*., 2015).

The feedback part of the CACC system can be considered as an ACC system. The acceleration of the preceding vehicle is received by the ego vehicle with a time delay of β which is due to the wireless communication delay between the two vehicles. The error signal (e_{i}) of the feedback control system shown in Figure 2 is the difference between the actual and desired relative distance and can be written as:

$$e_{\mathrm{i}} = d_{\mathrm{i}} - d_{\mathrm{r,i}} = x_{\mathrm{i-1}} - x_{\mathrm{i}} - \dot{x}_{\mathrm{i}} t_{\mathrm{hd,i}} \tag{7}$$

and the feedback path transfer function is $H_{\mathrm{i}}(s) = 1 + t_{\mathrm{hd,i}} s$

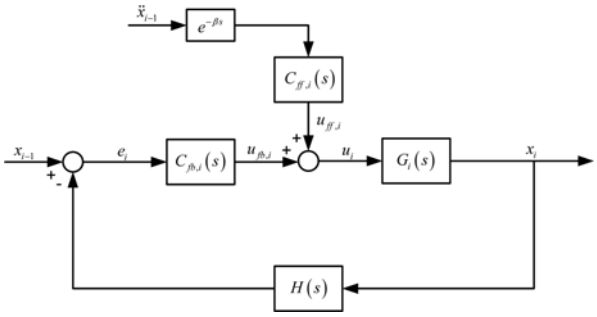

Figure 2. CACC system structure for a single vehicle.

and is used to implement the spacing policy given by Equation (4) with zero standstill distance.

3.1. Feedback Control System

PD type controllers can be used as the lower level feedback control $C_{fb,i}(s)$ of CACC systems since distance and speed signals used as feedback signals and the closed loop system has free integrators in the forward path. Here, the parameter space approach based robust control design methodology is applied to find the robust PD coefficients which satisfy D-stability design requirements. The design methodology can be summarized as follows.

Consider the plant $G(s)$ taken as the simple longitudinal vehicle model with spacing policy given by

$$G(s) = G_i(s)H(s) = \frac{N(s)}{D(s)} \tag{8}$$

where $N(s)$ represents the numerator of the plant and $D(s)$ represents its denominator. The real and imaginary parts of the numerator and denominator can be defined as

$$N(j\omega) = N_R(\omega) + jN_I(\omega) \text{ and}$$
$$D(j\omega) = D_R(\omega) + jD_I(\omega).$$

The PD controlled closed loop system characteristic equation can be written as

$$\begin{aligned} p_c(s) &= D(s) + (k_p + k_d s)N(s) \\ &= a_{n+1}s^{n+1} + a_n s^n + \ldots\ldots + a_1 s + a_0 = 0 \end{aligned} \tag{9}$$

where n is the degree of the plant $G(s)$.

The Hurwitz stability boundary crossed by a pair of complex conjugate roots is characterized by the following equations:

$$\begin{aligned} &\mathrm{Re}\left[p_c(j\omega)\right] = 0 \\ &\mathrm{Im}\left[p_c(j\omega)\right] = 0 \text{ for } \forall\omega \in (0,\infty). \end{aligned} \tag{10}$$

This is called the complex root boundary (CRB).

There may be a real root boundary such that a single real root crosses the boundary at frequency $\omega = 0$ which is characterized by

$$p_c(0) = 0 \quad \text{or} \quad a_0 = 0 \tag{11}$$

This is called the real root boundary (RRB).

There may exist an infinite root boundary (IRB) which is characterized by a degree drop in the characteristic polynomial at $\omega = \infty$. This degree drop in the characteristic polynomial is characterized as

$$a_{n+1} = 0 \tag{12}$$

in the characteristic polynomial in Equation (9). CRB, RRB and IRB solutions are obtained in the parameter space method of robust control by plotting the solutions of Equation (10) to Equation (12) parameterized by frequency ω in the k_p-k_d PD feedback controller parameter plane to show the Hurwitz stability regions of the given closed loop system. The specific controller parameter pair k_p-k_d that provides Hurwitz stability can be chosen visually within the stable region obtained in the controller parameter plane.

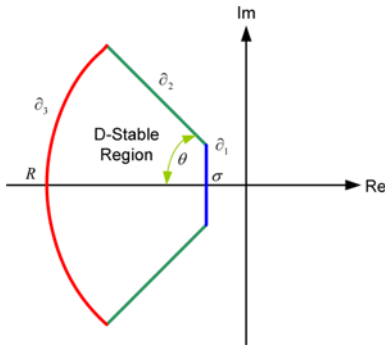

Figure 3. D-stable region in the complex plane.

The aforementioned parameter space computation method to determine Hurwitz stability regions can be extended to specify relative stability regions such as D-stability. A closed loop system is D-stable when the roots of the closed loop characteristic equation lie in the D-stable region in the complex plane as shown in Figure 3.

The average first order lag τ_i of the simple longitudinal vehicle model Equation (3) is taken as 0.5 sec here. In this paper, this value is considered to be an uncertain parameter changing between 0.3 and 0.7 sec ($\tau_{min} = 0.3 \le \tau_i \le \tau_{max} = 0.7$). D-stability requirements were determined as follows: no roots can be closer than – 0.5 to the imaginary axis ($\sigma = 0.5$) and no roots can be further than – 12 ($R = 12$), the maximum damping ratio can be $\zeta = 0.707$ which corresponds to $\theta = 45°$ in Figure 3.

The aim of the CACC system is to enable the use of shorter time gap settings as compared to ACC in the range of 0.6 sec to 1.1 sec (Bu *et al*., 2010). Figures 4 and 5 show the D-stability boundaries in parameter space corresponding to τ_{min} and τ_{max}, respectively. These boundaries are calculated when the time gap is $t_{hd} = 0.6$ sec. The solution regions in Figures 4 and 5 are shown superimposed on each other in Figure 6. The small region of intersection shown in Figure 6 is the controller parameter space region where D-stability

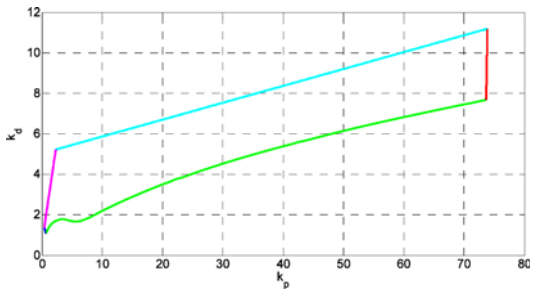

Figure 4. D-stability boundaries in parameter space for τ_{min}. (t_{hd} = 0.6 sec, blue line for ∂_1 CRB, magenta line for ∂_1 RRB, green line for ∂_2 CRB, red line for ∂_3 CRB and cyan line for ∂_3 RRB).

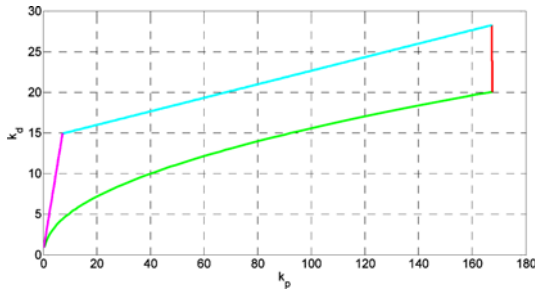

Figure 5. D-stability boundaries in parameter space for τ_{max}. (t_{hd} = 0.6 sec, blue line for ∂_1 CRB, magenta line for ∂_1 RRB, green line for ∂_2 CRB, red line for ∂_3 CRB and cyanide line for ∂_3 RRB).

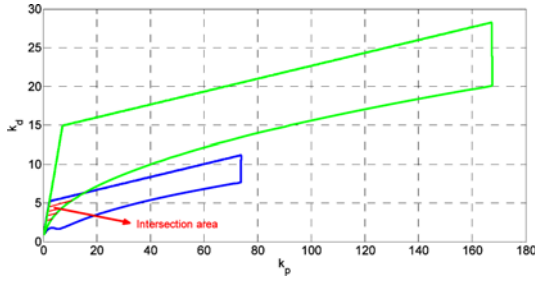

Figure 6. Common solution region for τ_{min} and τ_{max}.

is guaranteed for both the lower and upper bounds of the plant time constant. While not attempted here, the superimposition in Figure 6 is repeated for a large number of plant time constant values between the lower and upper limits.

Since the controller parameter space regions are dependent on the time gap, the computations presented above are repeated for several time gap values within the interval of 0.6 to 1.1 sec. It is then possible to use a three-dimensional plot to show the controller parameter space regions as a function of time gap. Consequently, Figures 7 and 8 show the D-stability boundaries in controller parameter space for lower and upper bounds of plant time constant τ_{min} and τ_{max} scheduled by time gap t_{hd}, respectively.

The PD controller parameters k_p and k_d to be used in the simulations presented in this paper were selected as 2 and 4, respectively, with t_{hd} = 0.6 sec from the intersection region shown in Figure 6. Note that this point satisfies the user selected D-stability requirements for all operating points between τ_{min} and τ_{max}. Figure 9 shows the closed loop system poles for τ_{min} and τ_{max}. It can be seen that closed loop system poles satisfy the D-stability requirements.

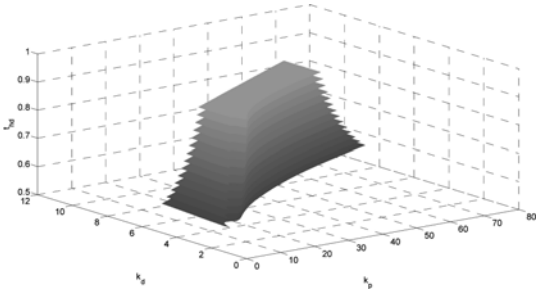

Figure 7. D-stability boundaries for lower bound of plant time constant τ_{min} scheduled by time gap t_{hd} ($0.6 \le t_{hd} \le 1.1$ sec).

3.2. Feedforward Control System

The second part of the CACC systems is the feedforward control, which is the main difference from an ACC implementation. In CACC systems, the acceleration of the preceding vehicle, which is obtained from the wireless communication with some communication delay, is used in the feedforward control system in order to obtain shorter time gaps than are possible with ACC systems. When the V2V communication link is disabled, the feedforward part of the control block diagram in Figure 2 vanishes and the CACC architecture naturally degenerates into the ACC architecture.

The aim of the feedforward control system is to make the error signal (e_i) zero. According to Figure 2, the transfer function between e_i and x_{i-1} can be written as follows:

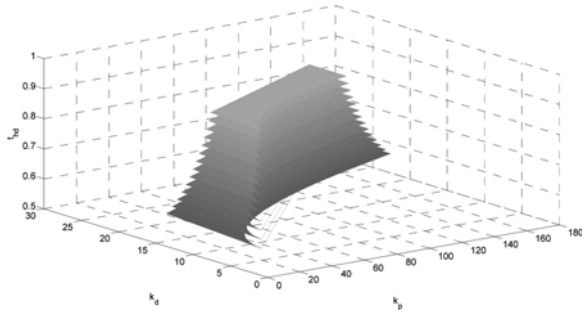

Figure 8. D-stability boundaries for upper bound of plant time constant τ_{max} scheduled by time gap t_{hd} ($0.6 \le t_{hd} \le 1.1$ sec).

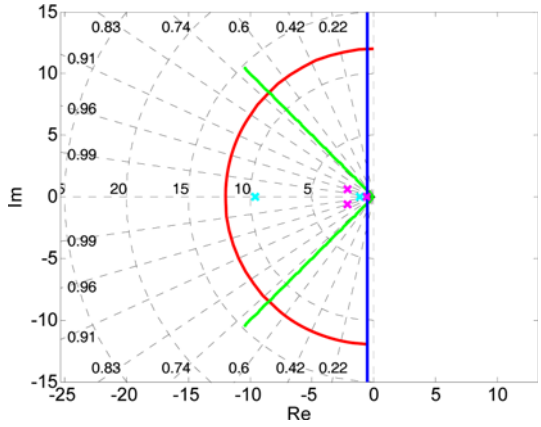

Figure 9. Closed loop system pole locations in the complex plane with the D-stability boundaries used (cyan cross for τ_{min} and magenta cross for τ_{max}).

$$\frac{E_i(s)}{X_{i-1}(s)} = \frac{1 - s^2 C_{ff,i}(s) G_i(s) H_i(s) e^{-\beta s}}{1 + C_{fb,i}(s) G_i(s) H_i(s)} \tag{13}$$

If the time delay effect ($e^{-\beta s}$) on the system is not taken into consideration in the design stage, the feedforward controller can be designed as is given below

$$1 - s^2 C_{ff,i}(s) G_i(s) H_i(s) = 0$$
$$\Rightarrow C_{ff,i}(s) = \frac{1}{s^2 G_i(s) H_i(s)} \tag{14}$$

which makes the error zero.

4. SIMULATION RESULTS

The parameter space based robust CACC design presented in the preceding sections is evaluated in simulation studies in this section. The simulation has a convoy of eight vehicles all under the CACC system in Figure 2 consisting of robust parameter space based feedback control and feedforward control given by Equation (14). The same simulations are also repeated with ACC given by the feedback controller in Figure 2 and the benchmark CACC system (Naus *et al*., 2010) only for comparison purposes. The benchmark CACC system by Naus *et al*. (2010) named as $CACC_1$ and the proposed parameter space approach based system named as $CACC_2$. $CACC_1$ system is a frequency domain based controller which consists of feedback and feedforward controllers. The feedback control structure for $CACC_1$ can be written as follows:

$$K(s) = k_p + k_d s = \omega_K (\omega_K + s) \tag{15}$$

where $k_p = k_d^2 = \omega_K$. ω_K shows the design frequency for the proposed controller. The feedforward control part is the same with $CACC_2$.

The desired time gap is 0.6 sec in both the ACC, $CACC_1$ and $CACC_2$ simulations. The V2V communication delay selected as 0.3 sec ($\beta = 0.3$) in the simulations. According to the results of Naus *et al*. (2010) for these time gap and communication delay configuration, ω_K should be selected as larger than 1.1 rad/sec for ensuring string stability. (Please, see Figure 9 in Naus *et al*. (2010) for more information). The value of ω_K is taken as 1.5 rad/sec in this study and the k_p and k_d values for the $CACC_1$ system are determined as 2.25 and 1.5, respectively.

As a summary, ACC is considered as feedback PD controller with $k_p = 2.25$ and $k_d = 1.5$, $CACC_1$ is considered as feedback PD and feedforward controller with $k_p = 2.25$ and $k_d = 1.5$ and $CACC_2$ is considered as feedback PD and feedforward controller with $k_p = 2$ and $k_d = 4$. The feedforward controller for $CACC_1$ and $CACC_2$ are taken as the same.

The simulation results are presented in Figures 10 ~ 12 for ACC, $CACC_1$ and $CACC_2$ controllers, respectively. This is a heterogeneous convoy of vehicles meaning that the models (time constant values) of all vehicles in the convoy are different and within the minimum and maximum bounds considered in the CACC design. Table 1 shows the different time constant values of the vehicles used in the simulations.

Table 1. Time constant values of the vehicles.

i	1	2	3	4	5	6	7	8
τ_i (s)	0.3	0.4	0.6	0.35	0.7	0.65	0.55	0.65

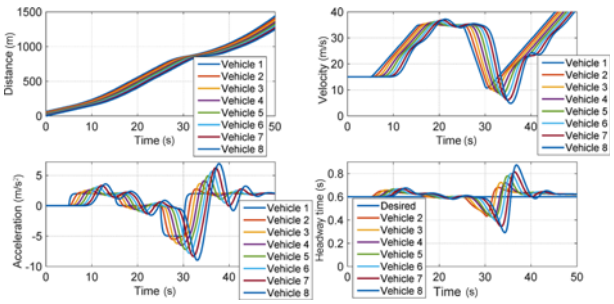

Figure 10. ACC simulation results for $\tau_{min} = 0.3 \le \tau_i \le \tau_{max} = 0.7$, heterogeneous traffic condition.

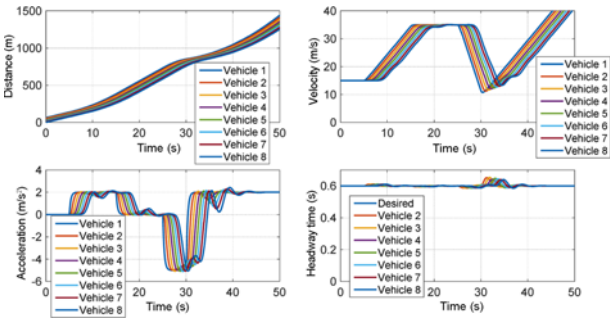

Figure 11. $CACC_1$ simulation results for $\tau_{min} = 0.3 \le \tau_i \le \tau_{max} = 0.7$, heterogeneous traffic condition.

The results include the displacement, velocity, acceleration and time gap plots. A comparison of the achieved time gaps in Figure 10 ~ 12 show the oscillatory response of the convoy with very poor time gap regulation in the ACC case whereas the corresponding time gap regulation in the CACC cases are much better. The acceleration oscillations in Figure 10 show that ACC also has poor drivability characteristics as compared to CACCs. Among CACC systems, $CACC_2$ shows better time gap regulation and less oscillatory motion in velocity and acceleration.

The same simulation for the $CACC_2$ system was repeated considering sensor noise. A band limited white noise was added to the position and the acceleration signals transmitted between the vehicles to represent the sensor noise originating from the radar sensor and the V2V communication system. The effect of the sensor noise on the signals can be seen in Figure 13. Although the

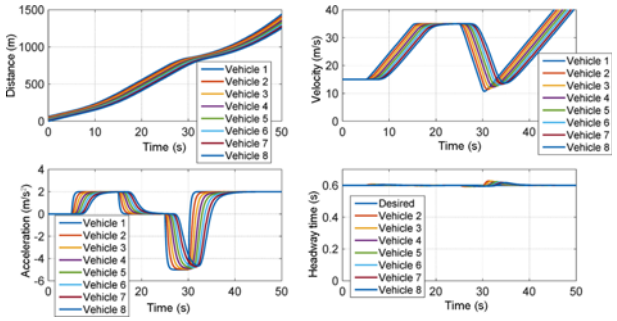

Figure 12. $CACC_2$ simulation results for $\tau_{min} = 0.3 \leq \tau_i \leq \tau_{max} = 0.7$, heterogeneous traffic condition.

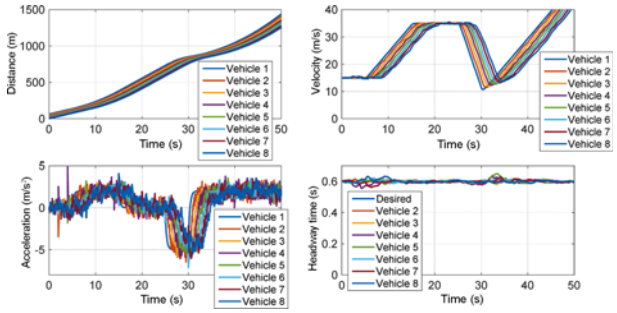

Figure 13. Sensor noise added $CACC_2$ simulation results for $\tau_{min} = 0.3 \leq \tau_i \leq \tau_{max} = 0.7$, heterogeneous traffic condition.

performance of the $CACC_2$ system deteriorated with the sensor noise, the desired time gap was still satisfied on average with an additional low amplitude oscillatory behavior.

5. EVALUATION OF COOPERATIVE ADAPTIVE CRUISE CONTROL SYSTEMS

Evaluation of ACC and CACC performance is carried out using time gap regulation based on time domain results and string stability based on frequency responses. Also, the effect of V2V communication frequency is investigated.

5.1. Time Gap

As the main aim of ACC and CACC systems is precise time gap regulation between vehicles in a convoy, these results corresponding to Figure 10 ~ 12 are presented in tabular format in Table 2. The RMS time gap tracking errors in Table 2 shows that $CACC_2$ is better by an order of magnitude as compared to ACC and $CACC_1$. The variance in the time gap values is also much smaller in $CACC_2$ as compared to ACC and $CACC_1$ which is also evident by a visual inspection of Figures 10 ~ 12. It is also seen that $CACC_1$ shows better performance than ACC which is expected.

Table 2. Comparison of time gap values of ACC, $CACC_1$ and $CACC_2$ systems for heterogeneous traffic condition.

	Desired	ACC	$CACC_1$	$CACC_2$
Minimum t_{hd} (sec)	0.6	0.3926	0.5867	0.5934
Average t_{hd} (sec)	0.6	0.6089	0.6012	0.6010
Maximum t_{hd} (sec)	0.6	0.7705	0.6451	0.6213
Average t_{hd} error (sec)	0	0.0089	0.0012	0.0010
RMS t_{hd} error (sec)	0	0.0614	0.0077	0.0047

5.2. String Stability

String stability is an important evaluation criterion for ACC and CACC systems. The string stability of a string of vehicles refers to the property in which spacing errors are guaranteed to attenuate as they propagate towards the tail of the string (Naus *et al*., 2010; Swaroop, 1995; Swaroop and Hedrick, 1996). It can be defined as follows:

$$\left\| SS_i(s) \right\|_\infty \leq 1 \Leftrightarrow \left| \frac{X_i(j\omega)}{X_{i-1}(j\omega)} \right| \leq 1, \ \forall \omega \tag{16}$$

Note that this is called strong string stability. The string stability transfer functions for ACC and CACC systems can be written using the block diagram representation of the system shown in Figure 2.

$$SS_{ACC,i}(s) = \frac{C_{fb,i}(s)G_i(s)}{1 + C_{fb,i}(s)G_i(s)H_i(s)} \tag{17}$$

$$SS_{CACC,i}(s) = \frac{(C_{fb,i}(s) + s^2 e^{-\beta s} C_{ff,i}(s))G_i(s)}{1 + C_{fb,i}(s)G_i(s)H_i(s)} \tag{18}$$

Both string stability transfer functions for each vehicle in the convoy are plotted as magnitude frequency response functions in Figure 14. The blue lines show the ACC equipped vehicles, the green lines show the $CACC_1$ equipped vehicles and the magenta lines show the $CACC_2$ equipped vehicles.

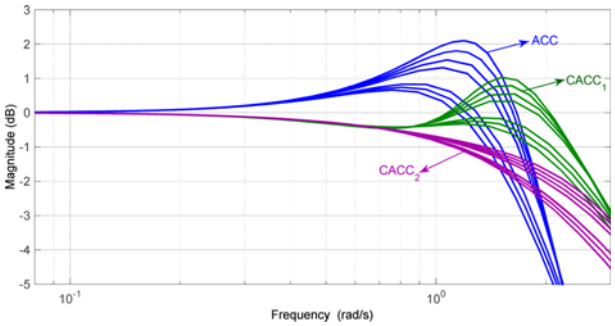

Figure 14. String stability transfer function frequency responses for ACC, $CACC_1$ and $CACC_2$ systems.

Table 3. Infinity norms of the string stability functions for ACC, $CACC_1$ and $CACC_2$ systems.

Vehicle, i	$\|SS_{ACC,i}\|_\infty$	$\|SS_{CACC_1,i}\|_\infty$	$\|SS_{CACC_2,i}\|_\infty$
1	1.0777	0.9999	0.9999
2	1.0991	1.0000	0.9999
3	1.1933	1.0691	0.9999
4	1.0873	1.0000	0.9999
5	1.2689	1.1247	0.9999
6	1.2305	1.0973	1.0000
7	1.1603	1.0439	1.0000
8	1.2305	1.0973	1.0000

The infinity norms of these string stability transfer functions for each vehicle are calculated and given in Table 3. The results show the improvement in string stability offered by $CACC_2$ over ACC and $CACC_1$. This improvement corresponds to the ACC and $CACC_1$ norm being larger than unity below 2 rad/sec whereas the $CACC_2$ norm is slightly below unity or unity in that frequency range (see Figure 14). Note that it is seen that $CACC_1$ system design improves the string stability with respect to ACC but it does not guarantee the string stability for all the vehicles in the convoy. The best string stability results are obtained by $CACC_2$ system.

5.3. V2V Communication Frequency

CACC differs from ACC by the use of acceleration information in the control system via V2V communication. V2V communication performance affects the performance of the system response. In order to test the effect of the V2V frequency, several simulation studies were performed. Table 4 shows the effect of V2V frequency on time gap regulation performance. It is seen that the time gap regulation performance decreases with the decrease of V2V frequency and there is no significant benefit of increasing the V2V frequency above 10 Hz for this maneuver. Figure 15 shows the $CACC_2$ simulation result

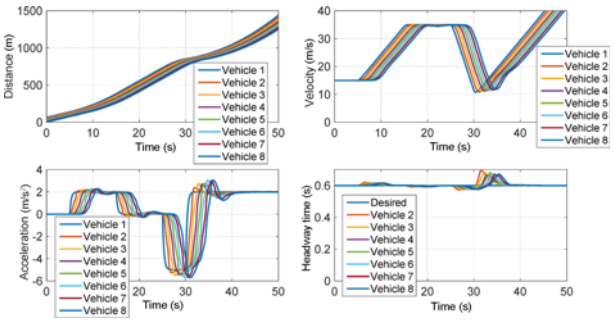

Figure 15. $CACC_2$ simulation results for $\tau_{min} = 0.3 \leq \tau_i \leq \tau_{max} = 0.7$, heterogeneous traffic condition with 1 Hz V2V communication frequency.

for 1 Hz V2V communication frequency (for the sake of brevity, only 1 Hz results were given in this paper). The shockwave effect on the velocity and acceleration signals can be seen from Figure 15, it is clear that the low selection of V2V frequency decreases the CACC system performance.

6. CONCLUSION

A robust parameter space based method for designing cooperative adaptive cruise control systems was developed and presented in this paper. The heterogeneous convoy simulation results demonstrated the usefulness of the method. The proposed $CACC_2$ design compared with ACC and the benchmark $CACC_1$ system by means of time gap and string stability analyses and the performance improvement of the $CACC_2$ system were shown in terms of these measures. Also, The designed controller tested in different conditions considering sensor noise and different frequencies of V2V communication. As a conclusion, it has been shown that the proposed robust control design methodology is straightforward and very implementable for CACC problem by considering uncertainties in vehicle model. Future work will concentrate on improving the design method, using phase margin and weighted sensitivity bounds in multi-objective design and using more realistic vehicle models in simulation.

Table 4. Comparison of time gap values for different V2V communication frequencies.

	Desired t_{hd} (sec)	V2V frequency					
		100 Hz	50 Hz	10 Hz	5 Hz	2 Hz	1 Hz
Minimum t_{hd} (sec)	0.6	0.5933	0.5932	0.5921	0.5908	0.5865	0.5762
Average t_{hd} (sec)	0.6	0.6010	0.6010	0.6012	0.6014	0.6019	0.6764
Maximum t_{hd} (sec)	0.6	0.6217	0.6221	0.6257	0.6300	0.6446	0.6029
Average t_{hd} error (sec)	0	0.0010	0.0010	0.0012	0.0014	0.0019	0.0029
RMS t_{hd} error (sec)	0	00048	0.0049	0.0056	0.0064	0.0091	0.0151

ACKNOWLEDGEMENT–The authors acknowledge the support of the Ohio State University Center for Automotive Research Industrial Consortium Intelligent Vehicles project (60047918).

REFERENCES

Ackermann, J., Blue, P., Bünte, T., Güvenç, L., Kaesbauer, D., Kordt, M., Muhler, M. and Odenthal, D. (2002). *Robust Control: The Parameter Space Approach.* Springer-Verlag London. London, UK.

Aksun Güvenç, B. and Kural, E. (2006). Adaptive cruise control simulator: A low-cost, multiple-driver-in-the-loop simulator. *IEEE Control Systems Magazine*, 42–55.

Bu, F., Tan, H.-S. and Huang, J. (2010). Design and field testing of a cooperative adaptive cruise control system. *American Control Conf. (ACC), IEEE,* Baltimore, MD, USA.

Choi, S. and Hedrick, J. K. (1995). Vehicle longitudinal control using an adaptive observer for automated highway systems. *American Control Conf. (ACC), IEEE*, Seattle,Washington, USA, 3106–3110.

Demirel, B. and Güvenç, L. (2010). Parameter space design of repetitive controllers for satisfying a robust performance requirement. *IEEE Trans. Automatic Control* **55**, **8**, 1893–1899.

Dey, K. C., Yan, L., Wang, X., Wang, Y., Shen, H., Chowdhury, M., Yu, L., Qui, C. and Soundararaj, V. (2016). A review of communication, driver characteristics, and controls aspects of cooperative adaptive cruise control (CACC). *IEEE Trans. Intelligent Transportation Systems* **17**, **2**, 491–509.

Gao, F., Dang, D. F., Huang, S. S. and Li, S. E. (2017). Decoupled robust control of vehicular platon with identical controller and rigid information flow. *Int. J. Automotive Technology* **18**, **1**, 157–164.

Güvenç, L. and Ackermann, J. (2001). Links between the parameter space and frequency domain methods of robust control. *Int. J. Robust and Nonlinear Control* **11**, **15**, 1435–1453.

Güvenç, L., Uygan, İ. M. C., Kahraman, K., Karaahmetoğlu, R., Altay, İ., Şentürk, M., Emirler, M. T., Hartavi Karcı, A. E., Aksun Güvenç, B., Altuğ, E., Turan, M. C., Taş, Ö. Ş., Bozkurt, E., Özgüner, Ü., Redmill, K., Kurt, A. and Efendioğlu, B. (2012). Cooperative adaptive cruise control implementation of team mekar at the grand cooperative driving challenge. *IEEE Trans. Intelligent Transportation Systems* **13**, **3**, 1062–1074.

Güvenç, L., Aksun Güvenç, B., Demirel, B. and Emirler, M. T. (2017). *Control of Mechatronic Systems.* The IET. London, UK.

Ioannou, P., Xu, Z., Eckert, S., Clemons, D. and Sieja, T. (1993). Intelligent cruise control: Theory and experiment. *Decision and Control, Proc. 32nd IEEE Conf.*, 1885–1890.

Kural, E. (2006). *Adaptive Cruise Control Design.* M. S. Thesis. Istanbul Technical University. Istanbul, Turkey.

Lidström, K., Sjöberg, K., Holmberg, U., Andersson, J., Bergh, F., Bjade, M. and Mak, S. (2012). A modular CACC system integration and design. *IEEE Trans. Intelligent Transportation System* **13**, **3**, 1050–1061.

Maschuw, J. P., Keßler, G. C. and Abel, D. (2008). LMI-based control of vehicle platoons for robust longitudinal guidance. *Proc. 17th IFAC World Cong.*, 12111–12116.

Naus, G. J., Vugts, R. P., Ploeg, J., van de Molengraft, M. J. and Steinbuch, M. (2010). String-stable CACC design and experimental validation: A frequency-domain approach. *IEEE Trans. Vehicular Technology* **59**, **9**, 4268–4279.

Ploeg, J., Semsar-Kazerooni, E., Lijster, G., van de Wouw, N. and Nijmeijer, H. (2015). Graceful degradation of cooperative adaptive cruise control. *IEEE Trans. Intelligent Transportation Systems* **16**, **1**, 488–497.

Rajamani, R. (2011). *Vehicle Dynamics Control.* Springer. New York, USA.

Swaroop, D. (1995). *String Stability of Interconnected Systems: An Application to Platooning in Automated Highway Systems*. Ph. D. Dissertation. University of California. Berkeley, USA.

Swaroop, D. and Hedrick, J. K. (1996). String stability of interconnected systems. *IEEE Trans. Automatic Control* **41**, **3**, 349–357.

Trudgen, M. and Mohammadpour, J. (2015). Robust cooperative adaptive cruise control design for connected vehicles. *Proc. ASME Dynamic Systems and Control Conf.*, Columbus, Ohio, USA.

Yanakiev, D., Eyre, J. and Kanellakopoulos, I. (1998). Longitudinal Control of Heavy Duty Vehicles: Experimental Evaluation. California PATH Research Report, UCB-ITS-PRR-98-15.